

Assignment V Array Impedance and Grating Lobes

EE4725 Quasi Optical Systems

Petar V. Peshev, p.v.peshev@student.tudelft.nl

*Department of Electrical Engineering, Mathematics, and Computer Science,
Delft University of Technology, Delft, The Netherlands*

Abstract

In this assignment, the input impedance in the E and H -planes is analyzed for two arrays with element spacing $d = 15$ mm and $d = 20$ mm respectively. The elements are spaced equally in the x and y -directions and consist of dipoles with width $W = 1$ mm and length $L = 14$ mm. Finally, the frequency of operation is $f = 10$ GHz.

I. SIMULATIONS

The scripts used to simulate the lens antenna are in the GIT repository Assignment V; and the library developed and used in the scripts is in quasi-optics-library. To run the simulations either place the script and library repositories in the same parent folder or change the library path in the simulation scripts.

II. INPUT IMPEDANCE

The input impedance of an array is

$$Z_{in} = -\frac{1}{d_x d_y} \sum_{m_x} \sum_{m_y} \bar{G}_{xx}^{EJ}(k_{xm}, k_{ym}) I^2(k_{xm}) J^2(k_{ym}), \quad (1)$$

where the impedance is related to the xx -component of the Spectral Green's functions and $I(k_{xm})J(k_{ym})$ is the basis function derived from the Fourier transform of the equivalent current distribution on the dipole element

$$B(k_{xm}, k_{ym}) = I(k_{xm})J(k_{ym}) = \frac{2k_0(\cos(\frac{k_{xm}L}{2}) - \cos(\frac{k_0L}{2}))}{(k_0^2 - k_{xm}^2) \sin(k_0 \frac{L}{2})} \text{sinc}(\frac{k_{ym}W}{2}), \quad (2)$$

and is related to the floquet modes. The input impedance is, in essence, the sum of the infinite floquet modes of the x -component (assuming the dipole is oriented along the x -direction) of the E -field times the Fourier transform of the basis function, and scaled by the spacing between the elements.

The input impedance of the array configuration with $d_x = d_y = 15$ mm spacing is plotted for the E , D , and H -planes in Fig.1, Fig.2, and Fig.3 respectively. At the E -plane, the real part of the impedance decreases as the elevation angle approaches $\theta = 90^\circ$; while, the imaginary part decreases until $\theta = 45^\circ$ and then increases as it approaches $\theta = 90^\circ$. At the H -plane, the real and imaginary parts of the impedance is constant in the neighbourhood at $\theta = 0^\circ$; however, they increase as the elevation angle approaches $\theta = 90^\circ$ where the impedance component goes to infinity. Furthermore, at the E -plane, $k_y = 0$ rad/m, thus, the m_y floquet modes only scale the impedance contributed by the respective m_y mode by $\text{sinc}(-m_y \pi W / d_y)$. Regarding the k_{xm} floquet modes, $k_x = k_0 \sin \theta$, therefore, the k_x maximum appears at $\theta = 90^\circ$ (equal to k_0); hence, as the elevation angle approaches $\theta = 90^\circ$, the $I(k_0)$ decreases to zero. On the other hand, at the H -plane, $k_x = 0$ rad/m, thus, $I(k_{xm})$ is scaling the basis (in a similar way as k_{ym} in the E -plane) and $J(k_{ym})$ again acts as a scaling factor as a function of θ and the m_y floquet mode. However, in the xx -component of the Spectral Green's function, $k_z \rightarrow 0$ as $\theta \rightarrow 90^\circ$ ($k_y \rightarrow k_0$) for the fundamental mode $m_y = 0$, consequently $\bar{G}_{xx}^{EJ} \rightarrow \infty$ (this singularity did not occur in the E -plane, because the $\lim_{k_x \rightarrow k_0} \bar{G}_{xx}^{EJ}$ does not go to ∞). The singularity in \bar{G}_{xx}^{EJ} at the H -plane causes a singularity in the H -plane of Z_{in} .

Consequently, the singularity appearing at the E -plane is not a strictly defined singularity but a minimum in the impedance; for an array with spacing $d_x = \lambda/2$, the $(m_x = 1, m_y = 0)$ floquet mode becomes visible at the $\theta \approx 90^\circ$, therefore the minimum value of the impedance approaches zero. At the H -plane, the singularity is caused by the input impedance going to infinity, as a consequence of the xx -component of the Spectral Green's function going to infinity. These effects (zero input impedance's real part at $\theta = 90^\circ$ at the E -plane and singularity at $\theta = 90^\circ$ at the H -plane) always appear for well sampled antenna arrays, $d \leq \lambda/2$.

The input impedance of the array configuration with $d_x = d_y = 20$ mm spacing is plotted for the E , D , and H -planes in Fig.4, Fig.5, and Fig.6 respectively. At the E -plane, the real part of the impedance decreases until it reaches a minimum at the grating lobe at $\theta = 30^\circ$ and then begins to increase until $\theta \approx 45^\circ$ at which point it again begins to decrease until it reaches

a second local minimum at $\theta = 90^\circ$ (in this case the minimum impedance's real part does not go to zero). At the H -plane, the real and imaginary parts of the impedance is overall constant in the neighbourhood of $\theta = 0^\circ$; however, at the grating lobe ($\theta = 30^\circ$), the impedance has a singularity, after which the imaginary part is constant while the real part decreases until $\theta \approx 50^\circ$ and after this point increases until it reaches its second singularity at $\theta = 90^\circ$. The causes of these minimums and singularities in the impedance at the E and H -planes is the same as for the causes in array with spacing $d_x = d_y = 15$ mm, however, the floquet modes entering the visible region increase the periodicity of the impedance (the increase and decrease in the impedance at the different planes repeat more often depending on the number of modes entering the visible region at these planes).

Consequently, the minimums appearing at the E -plane for the $d_x = d_y = 20$ mm spacing are at $\theta = 30^\circ$ (grating lobe) and at $\theta = 90^\circ$. While the singularities appearing at the H -plane for the same array are also at $\theta = 30^\circ$ and $\theta = 90^\circ$.

III. GRATING LOBES

The conditions ensuring the array does not have grating lobes are

$$k_{x0} \leq \frac{2\pi}{d_x} - k_0, \quad (3a)$$

$$k_{y0} \leq \frac{2\pi}{d_y} - k_0; \quad (3b)$$

as a consequence, the grating lobes at the E and H -plane ($k_{x0} = k_0 \sin \theta$ and $k_{y0} = 0$, and $k_{x0} = 0$ and $k_{y0} = k_0 \sin \theta$ respectively) are

$$\theta_{gr,E} = \sin^{-1}\left(\frac{\lambda}{d_x} - 1\right), \quad (4a)$$

$$\theta_{gr,H} = \sin^{-1}\left(\frac{\lambda}{d_y} - 1\right). \quad (4b)$$

Hence, the grating lobes at the E -plane is at $\theta_{gr,E} = 90^\circ$ and at the H -plane $\theta_{gr,H} = 90^\circ$ (assuming speed of light $c = 3 \cdot 10^8$ m/s) for an array with spacing $d_x = d_y = 15$ mm, and $\theta_{gr,E} = 30^\circ$ and $\theta_{gr,H} = 30^\circ$ for $d_x = d_y = 20$ mm. Grating lobes are not expected in the D -plane for both cases.

The grating lobe diagram for the antenna array with spacing $d_x = d_y = 15$ mm is plotted in Fig.7. The diagram confirms the analytical expectation of grating lobes at $\theta_{gr,E} = 90^\circ$ and $\theta_{gr,H} = 90^\circ$, and no grating lobes at the D -plane.

The grating lobe diagram for the antenna array with spacing $d_x = d_y = 20$ mm is plotted in Fig.8. The diagram confirms the analytical expectation of grating lobes at $\theta_{gr,E} = 30^\circ$ and $\theta_{gr,H} = 30^\circ$, and no grating lobes at the D -plane.

Array Impedance @ E-plane, $f = 10$ GHz, $L = 14$ mm, $W = 1$ mm, $d_x = 15$ mm, and $d_y = 15$ mm

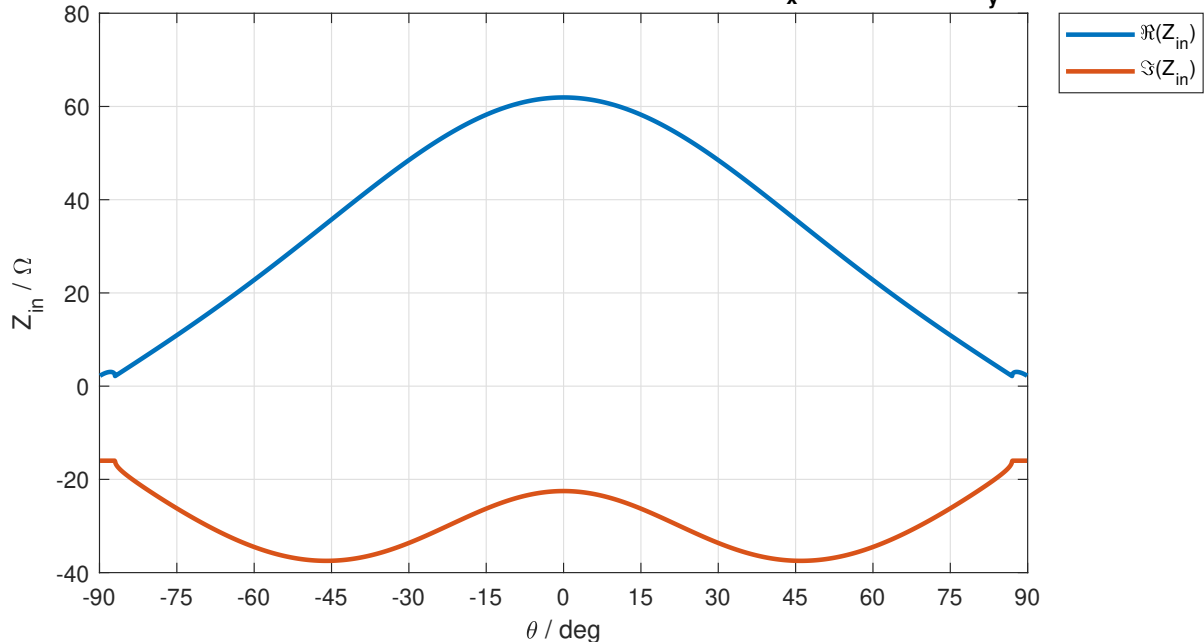


Fig. 1. Array impedance for $d_x = d_y = 15$ mm spacing, and dipole width $W = 1$ mm and length $L = 14$ mm, as a function of the elevation angle θ in the E -plane, $\phi = 0^\circ$ and 180° .

Array Impedance @ D-plane, $f = 10$ GHz, $L = 14$ mm, $W = 1$ mm, $d_x = 15$ mm, and $d_y = 15$ mm

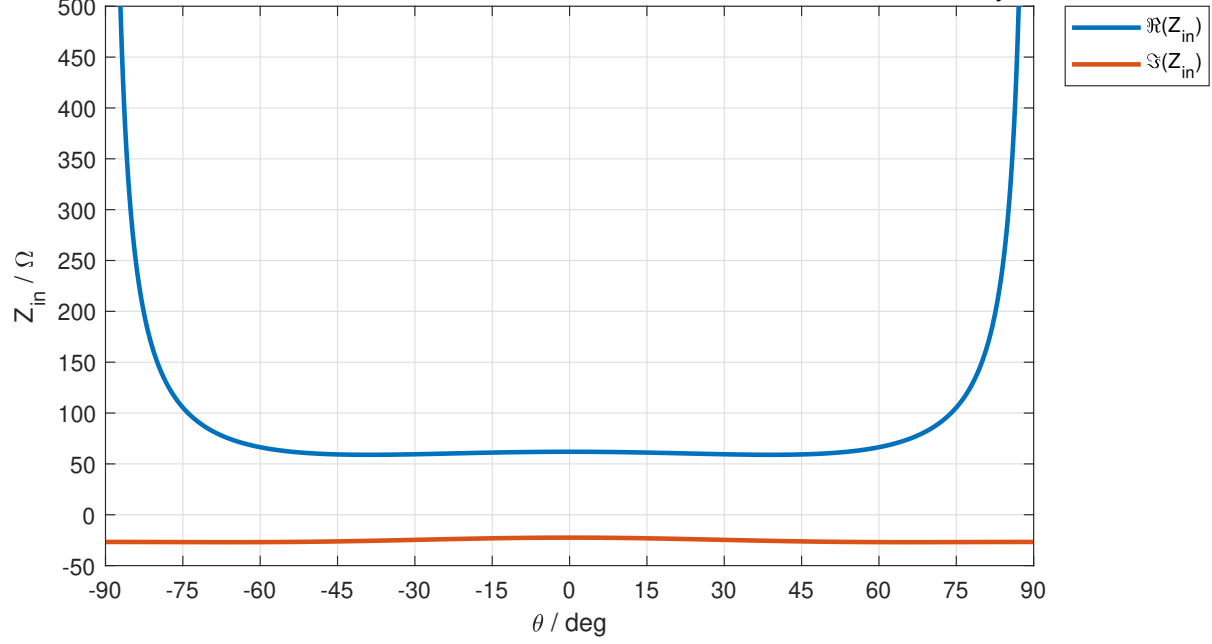


Fig. 2. Array impedance for $d_x = d_y = 15$ mm spacing, and dipole width $W = 1$ mm and length $L = 14$ mm, as a function of the elevation angle θ in the H -plane, $\phi = 45^\circ$ and 225° .

Array Impedance @ H-plane, $f = 10$ GHz, $L = 14$ mm, $W = 1$ mm, $d_x = 15$ mm, and $d_y = 15$ mm

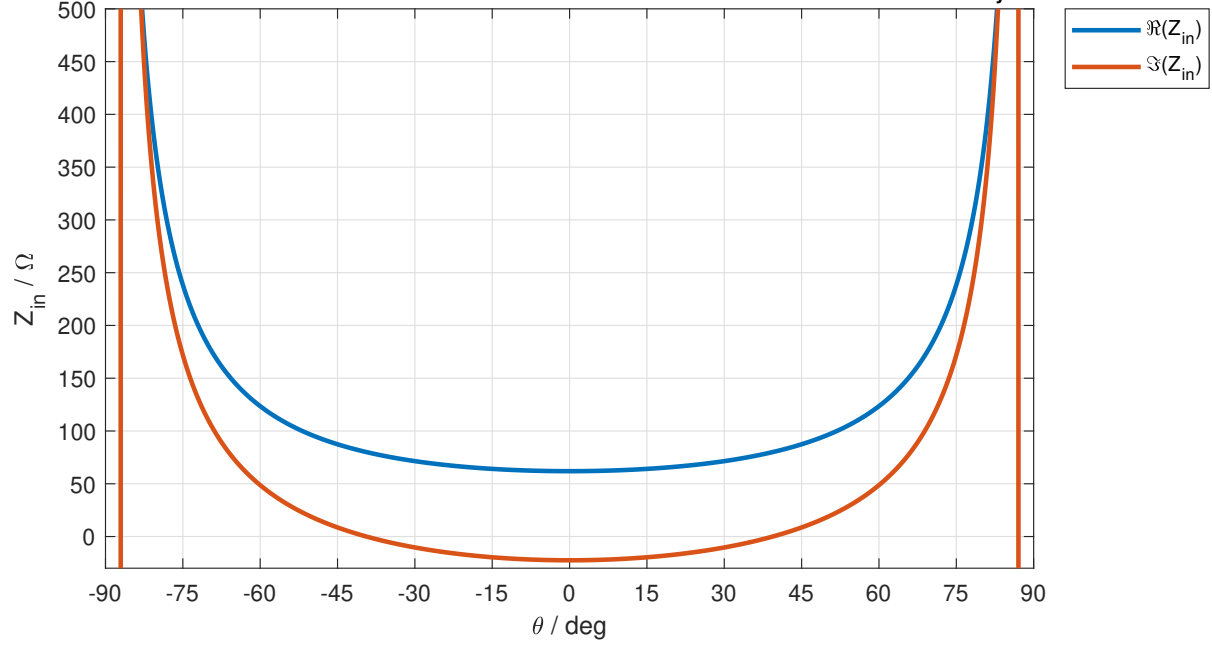


Fig. 3. Array impedance for $d_x = d_y = 15$ mm spacing, and dipole width $W = 1$ mm and length $L = 14$ mm, as a function of the elevation angle θ in the H -plane, $\phi = 90^\circ$ and 270° .

Array Impedance @ E-plane, $f = 10$ GHz, $L = 14$ mm, $W = 1$ mm, $d_x = 20$ mm, and $d_y = 20$ mm

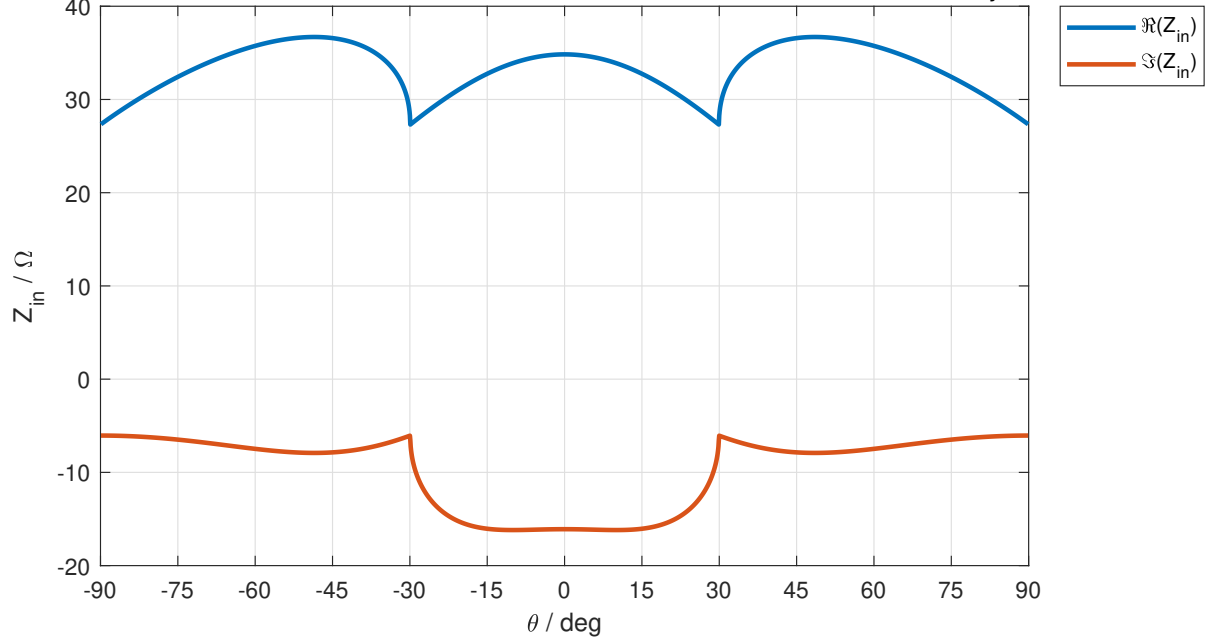


Fig. 4. Array impedance for $d_x = d_y = 20$ mm spacing, and dipole width $W = 1$ mm and length $L = 14$ mm, as a function of the elevation angle θ in the E -plane, $\phi = 0^\circ$ and 180° .

Array Impedance @ D-plane, $f = 10$ GHz, $L = 14$ mm, $W = 1$ mm, $d_x = 20$ mm, and $d_y = 20$ mm

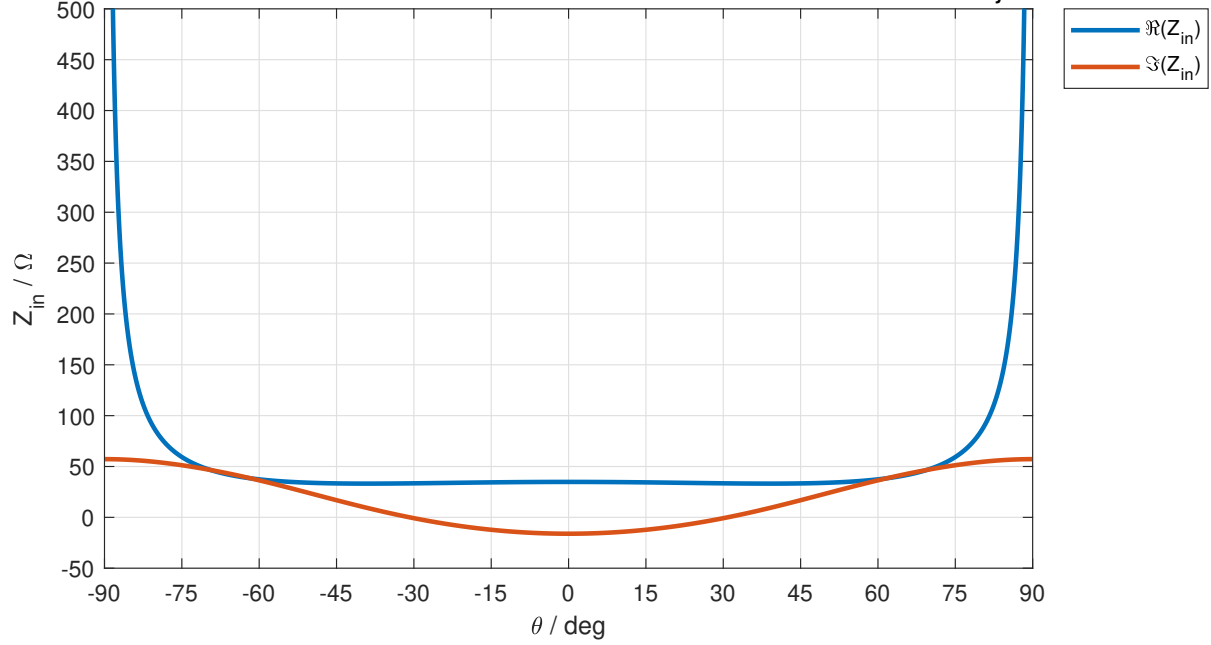


Fig. 5. Array impedance for $d_x = d_y = 20$ mm spacing, and dipole width $W = 1$ mm and length $L = 14$ mm, as a function of the elevation angle θ in the H -plane, $\phi = 45^\circ$ and 225° .

Array Impedance @ H-plane, $f = 10$ GHz, $L = 14$ mm, $W = 1$ mm, $d_x = 20$ mm, and $d_y = 20$ mm

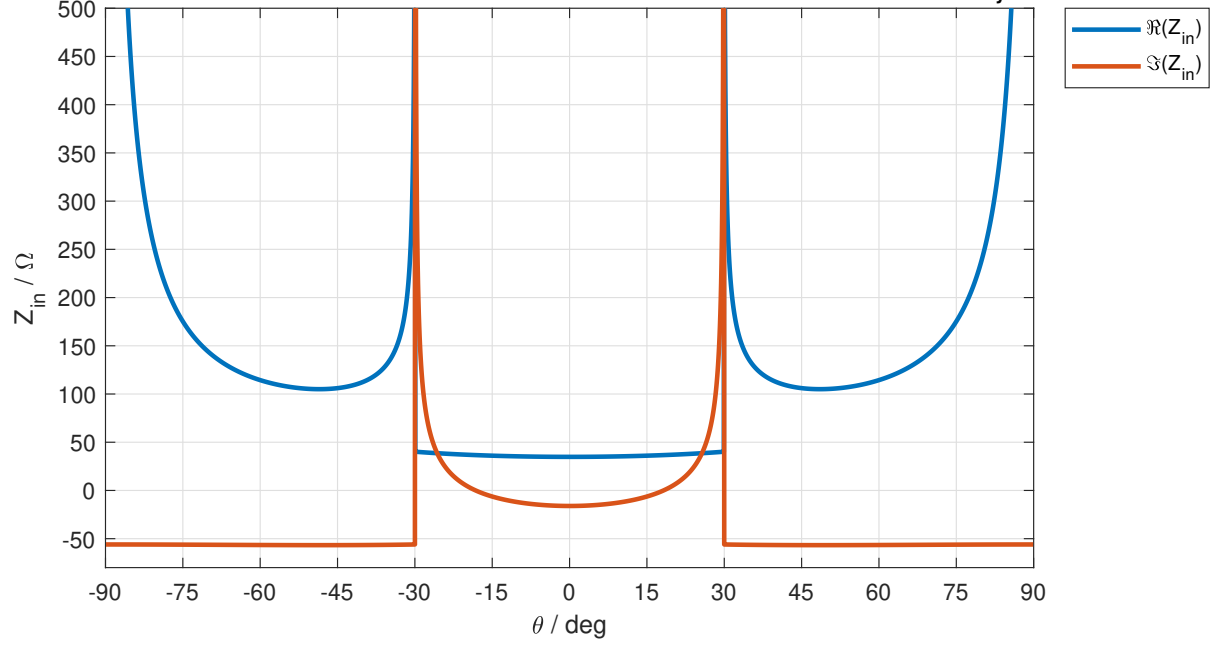


Fig. 6. Array impedance for $d_x = d_y = 20$ mm spacing, and dipole width $W = 1$ mm and length $L = 14$ mm, as a function of the elevation angle θ in the H -plane, $\phi = 90^\circ$ and 270° .

Grating Lobes @ $f = 10$ GHz, $d_x = 15$ mm, and $d_y = 15$ mm

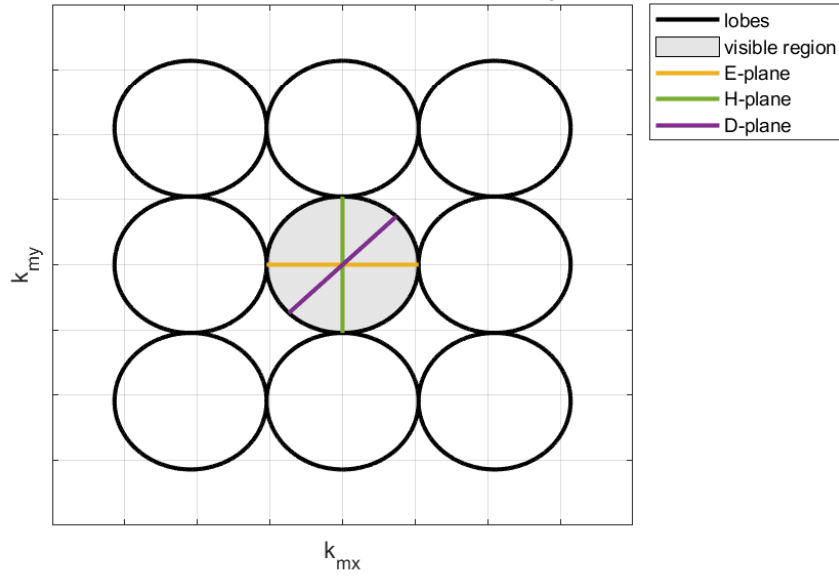


Fig. 7. Grating lobe diagram for the array configuration with spacing $d = 15$ mm; the E and H -planes are marked with yellow and green respectively.

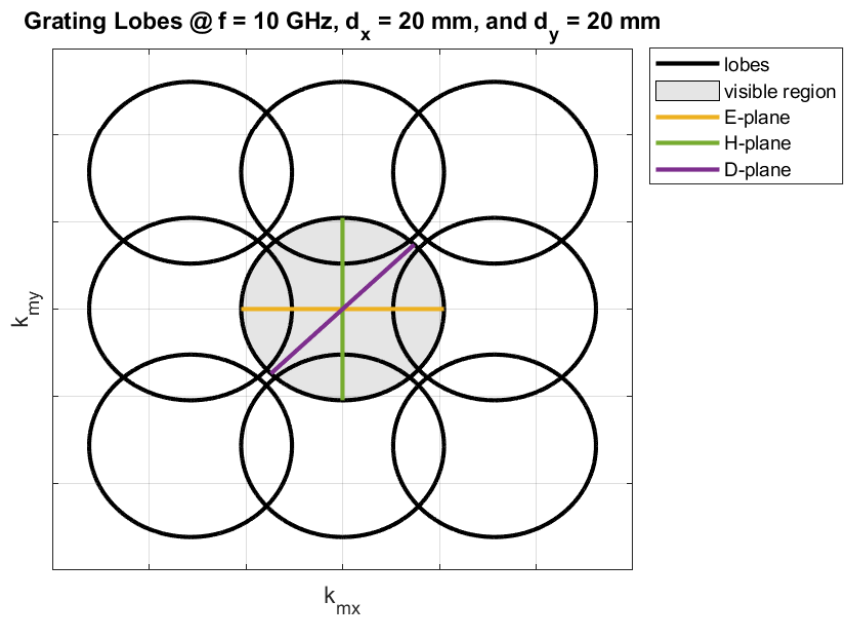


Fig. 8. Grating lobe diagram for the array configuration with spacing $d = 20$ mm; the E and H -planes are marked with yellow and green respectively.